Available online at www.sciencedirect.com
ScienceDirect
Developmental Biology 300 (2006) 512–522
DEVELOPMENTAL BIOLOGY
www.elsevier.com/locate/ydbio

On the role of glypicans in the process of morphogen gradient formation

Lars Hufnagel [a,1], Johan Kreuger [b,1], Stephen M. Cohen [c], Boris I. Shraiman [a,*]

[a] *Kavli Institute for Theoretical Physics, Kohn Hall, University of California, Santa Barbara, CA 93106, USA*
[b] *Department of Genetics and Pathology, Uppsala University, Rudbeck Laboratory, Dag Hammarskjöldsv. 20, SE-75185 Uppsala, Sweden*
[c] *European Molecular Biology Laboratory, Meyerhofstrasse 1, 69117 Heidelberg, Germany*

Received for publication 12 October 2005; revised 13 August 2006; accepted 30 August 2006
Available online 19 September 2006

Abstract

Glypicans are cell surface molecules that influence signaling and gradient formation of secreted morphogens and growth factors. Several distinct functions have been ascribed to glypicans including acting as co-receptors for signaling proteins. Recent data show that glypicans are also necessary for morphogen propagation in the tissue. In the present study, a model describing the interaction of a morphogen with glypicans is formulated, analyzed and compared with measurements of the effect of glypican Dally-like (Dlp) overexpression on Wingless (Wg) morphogen signaling in *Drosophila melanogaster* wing imaginal discs. The model explains the opposing effect that Dlp overexpression has on Wg signaling in the distal and proximal regions of the disc and makes a number of quantitative predictions for further experiments. In particular, our model suggests that Dlp acts by allowing Wg to diffuse on cell surface while protecting it from loss and degradation, and that Dlp rather than acting as Wg co-receptor competes with receptors for morphogen binding.

Keywords: Wingless; Dally-like; Glypican; Morphogen; Diffusion; Gradient

Introduction

One of the profound insights into the mechanisms of animal development gained over last decades of work is the demonstration of the key role of morphogen gradients in spatial patterning of animal bodies, organs and limbs. "Morphogen gradients" are graded distributions of certain diffusible proteins, which regulate expression of numerous target genes in a concentration dependent manner (for a recent review, see Tabata and Takei, 2004). Although the existence of various morphogen gradients and their role is now firmly established, the mechanisms that generate and regulate these gradients are still not understood. An excellent experimental model of morphogen action is provided by imaginal discs of *Drosophila melanogaster* larvae, which are the precursors of adult fly organs and limbs (Held, 2002). Here we will focus on wing imaginal discs and examine the role of glypicans in the formation of morphogen gradients.

The *Drosophila* wing imaginal disc is derived from the embryonic ectoderm and is composed of two cell layers: the columnar epithelium and the peripodial epithelium. The columnar epithelium in the wing pouch of the wing disc (Fig. 1) will give rise to the wing blade in the adult fly. Patterning of this tissue is organized by two morphogens Wingless (Wg) and Decapentaplegic (Dpp) (Brook and Cohen, 1996; Lawrence and Struhl, 1996; Tabata and Takei, 2004). Wg is secreted by cells at the boundary of dorsal and ventral compartments, whereas Dpp is secreted by cells adjacent to the antero-posterior boundary. Signaling by both Wg and Dpp is known to depend on surface glypicans Dally and Dally-like (Dlp) (Belenkaya et al., 2004; Fujise et al., 2001; Han et al., 2005; Jackson et al., 1997; Kreuger et al., 2004; Lin and Perrimon, 1999, 2000; Perrimon and Bernfield, 2000; Selleck, 2001; Tsuda et al., 1999), which modulate the levels and the spatial distribution of morphogens and thus play a major role in the establishment of morphogen gradients.

Dlp and Dally belong to the large family of heparan sulfate (HS) proteoglycans, which are present on the surface of all adherent cells, as well as in the extracellular matrix, and

* Corresponding author.
E-mail address: shraiman@kitp.ucsb.edu (B.I. Shraiman).
[1] Contributed equally to this study.

0012-1606/$ - see front matter © 2006 Elsevier Inc. All rights reserved.
doi:10.1016/j.ydbio.2006.08.076

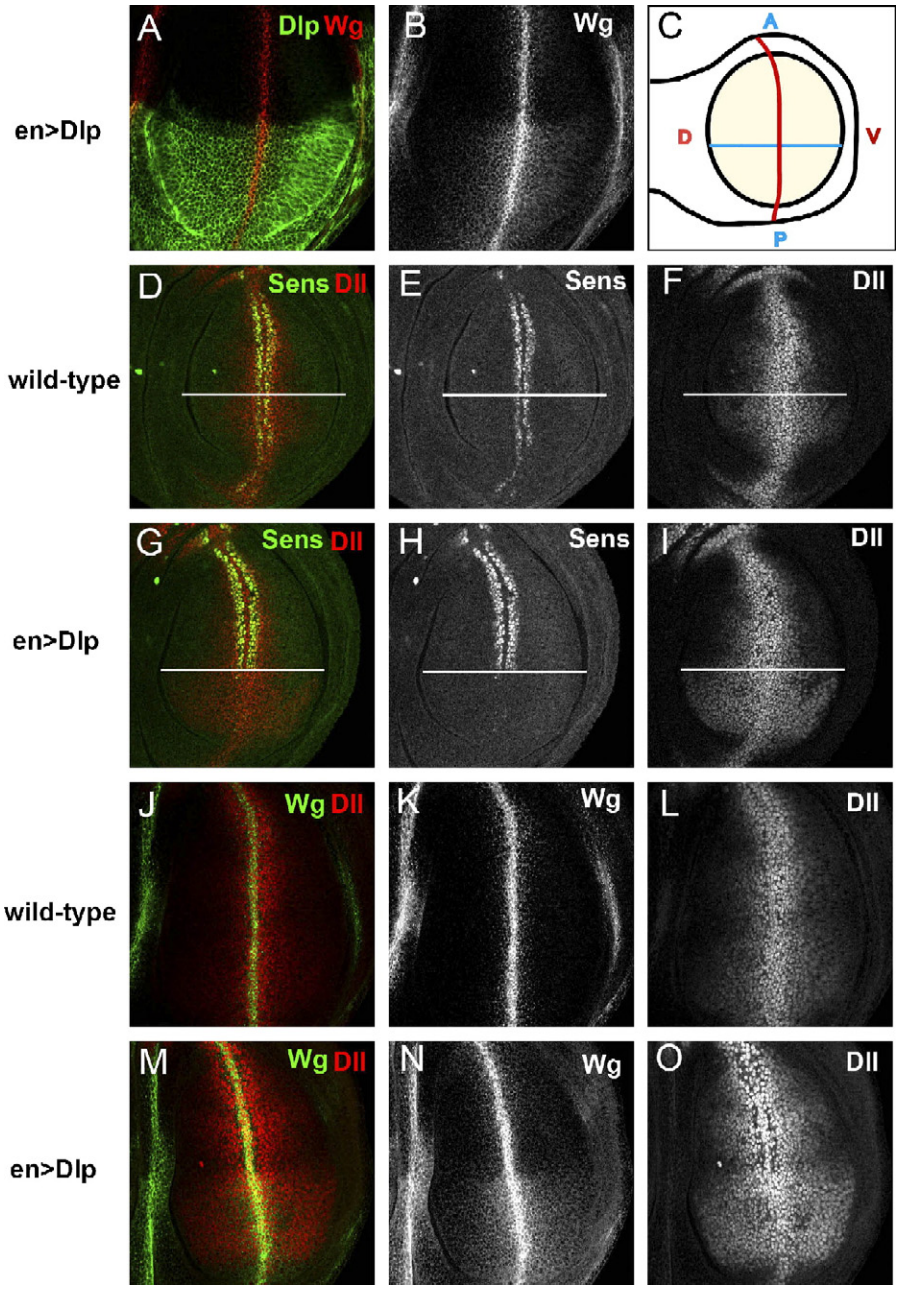

Fig. 1. Signaling by Wg in the *D. melanogaster* wing imaginal disc is modulated by Dlp. (A, B) Disc overexpressing Dlp in the posterior compartment under the control of the engrailed promoter, stained for Dlp and Wg. (C) Cartoon of a wing imaginal disc. The wing pouch, where Wg-signaling was recorded, is shown in yellow. The blue line corresponds to the boundary between anterior (top) and posterior (bottom) compartments. The red line corresponds to the stripe of Wg producing cells at the dorso-ventral border. (D–F) Wild-type discs, stained for Wg target genes: Sens is induced only by high levels of Wg, close to the DV boundary, whereas Dll is induced also by intermediate levels of Wg. (G–I) A disc overexpressing Dlp stained for Sens and Dll. Note that Sens expression is inhibited by increased levels of Dlp, whereas the Dll expression domain is expanded at the dorsal and ventral ends of the wing pouch (see also Franch-Marro et al., 2005). (J–L) Wild-type disc stained for Wg and Dll. (M–O) Discs overexpressing Dlp stained for Wg and Dll.

modulate the activities of a large number of protein ligands including growth factors and morphogens (Bernfield et al., 1999). More than 100 proteins have been reported to interact with the HS moiety of proteoglycans. HS is a linear polysaccharide of glycosaminoglycan type expressing a multitude of sulfated epitopes that constitute binding sites for protein ligands (Esko and Lindahl, 2001). Two major types of cell-surface-bound proteoglycan core proteins have been identified: the transmembrane syndecans and the glycosylphosphoinositide-linked glypicans. Both syndecans and glypicans are thought to be expressed in high copy numbers (10^6 per cell) (Bernfield et al., 1992). HSPGs have been suggested to function as co-receptors for growth factors (e.g., fibroblast growth factors) facilitating formation of active receptor complexes (Franch-Marro et al., 2005; Pellegrini et al., 2000; Yayon et al., 1991).

The present study is focused on Wingless (Wg) signaling and its dependence on Dally-like (Dlp), which has been observed to

modulate Wg activity, as measured by levels of Senseless (Sens), a Zn finger transcription factor required for the development of the peripheral nervous system, and Distal-less (Dll), a leg selector gene (Giraldez et al., 2002; Kreuger et al., 2004). Fig. 1 presents a sample of fluorescent images visualizing distributions of Wg, Dll and Sens in wing imaginal discs (isolated at the end of the 3rd larval instar) from wild-type (WT) flies, and flies which overexpress Dlp selectively in the posterior compartment under the control of the Engrailed (*en*) promoter (*en*Gal4>Dlp). Dlp is known to act as a *positive cofactor* to increase Wg activity in the regions of the wing disc distant from the site of Wg production at the dorso-ventral (DV) boundary. Surprisingly, Dlp also acts as a *negative cofactor* suppressing Wg activity near the DV boundary, where Wg levels are the highest (Baeg et al., 2004; Kirkpatrick et al., 2004; Kreuger et al., 2004) as shown in Fig. 2. This "contradictory" effect of Dlp confounds simple intuitive explanations. Below we shall show that this behavior would follow if the primary role of Dlp were to retain Wg on the cell surface, instead of acting as a conventional co-receptor required for interaction between Wg and its high affinity receptors—the proteins of the Frizzled family (Orsulic and Peifer, 1996). Quantitative understanding of the effect of Dlp on Wg distribution and activity can be achieved with the help of a simple model of morphogen diffusion in the presence of glypicans and receptors on cell surface. The purpose of this report is to formulate and analyze such a model.

Models of morphogen gradient formation have been previously considered by a number of workers. Kerszberg and Wolpert (1998) argued that binding to receptors precludes formation of a stable morphogen gradient (by diffusion) giving rise instead to a propagating front of saturated receptors. This conclusion was challenged by Lander et al. (2002) who simulated a model of a diffusible ligand binding to receptors and concluded that receptors impede, but not preclude gradient formation. Lander et al. also used numerical simulations to critically reevaluate the evidence for *trans*-cytosis (Entchev et al., 2000) concluding that it is in fact consistent with passive diffusion as the mechanism of morphogen transport. This conclusion was reinforced by subsequent experiments of Belenkaya et al. (2004). The general framework for interpreting perturbations of morphogen profiles induced by mutant clones, of the type used in the experiments of Entchev et al. (2000) and Belenkaya et al. (2004) was provided recently by Eldar and Barkai (2005). In another interesting series of papers Eldar, Barkai and coworkers (Eldar et al., 2002, 2003, 2004) pointed out that cooperative effects in degradation of morphogens have a dramatic effect on its spatial distribution

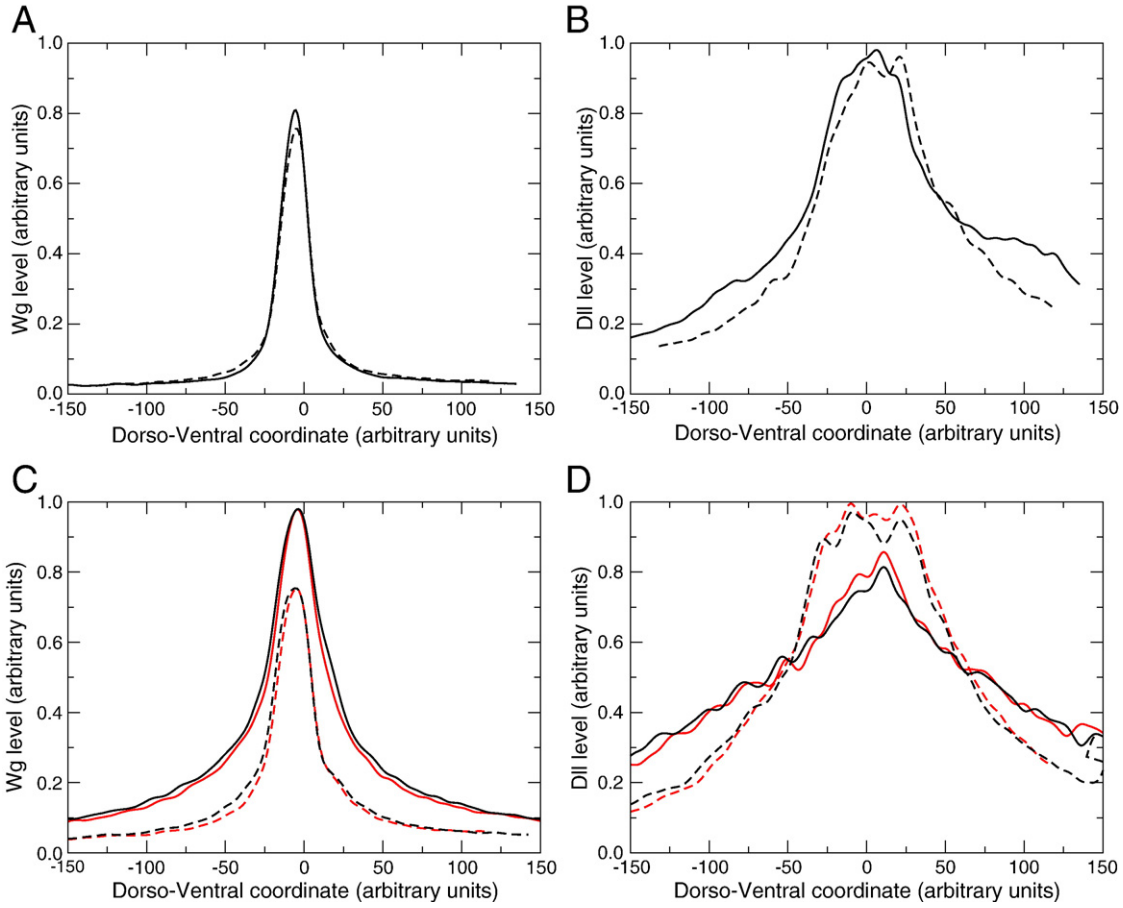

Fig. 2. Wg and Dll profiles in wing imaginal discs. Measured Wg profiles (A) and corresponding Dll profiles (B) in a wild-type wing imaginal disc. Dashed and solid lines indicate anterior and posterior compartments of the wing pouch, respectively. (C, D) Wg profiles and corresponding Dll expression profiles in two different wing discs that overexpress Dlp in the posterior compartment. Black and red lines represent different discs.

and quite generally lead to the creation of a region where morphogen gradient is independent of the variation in the rate of morphogen production at the source. This effect enhances the robustness of morphogen gradients. Surprisingly, despite the key role played by glypicans in controlling morphogen gradients, none of the above models described their role. Glypicans were considered in a recent model of morphogen spreading by Cinquin (2006). This model allows for the equilibration of extracellular morphogen with glypican-bound morphogen on cell surface but limits morphogen diffusion to the extracellular component. For reasons that shall be detailed below, it does not explain the observed effect of Dlp overexpression on Wg.

Below we will first formulate a model of glypican function in morphogen gradient formation, then present the results of model analysis and their comparison with experiment and finally discuss the conclusions of the analysis as well as specify some additional predictions of the model.

The model

Let us consider morphogen spreading by diffusion along the surface of a tissue layer while interacting with surface glypicans (Belenkaya et al., 2004) and receptors as illustrated in Fig. 3. A line of source cells (e.g., corresponding to the DV boundary, in the case of Wg) secretes morphogen W at a rate s (per unit length). Free morphogen can diffuse in the intercellular space with diffusivity D or reversibly bind a glypican, G, on the surface, forming W^*—the glypican-bound surface moiety of morphogen: $W+G \Leftrightarrow W^*$ (with forward and reverse rates k and k', respectively) (Belenkaya et al., 2004). We shall assume that the surface moiety W^* can still diffuse along the surface with diffusivity D^*. We shall assume that both free W and glypican-bound W^* morphogen moieties can reversibly bind and activate surface receptors, $W+R \Leftrightarrow R^*$ and $W^*+R \Leftrightarrow R_g^*$, resulting in the transduced morphogen signal proportional to the total number of ligand-bound receptors $R+R_g^*$. These processes are described quantitatively by a set of reaction–diffusion equations:

$$\frac{\partial}{\partial t}W(x,t) = D\frac{\partial^2}{\partial x^2}W(x,t) - \gamma W(x,t) - [kGW(x,t) - k'W^*(x,t)] - [k_R RW(x,t) - k_R' R^*(x,t)] + s\delta(x) \quad (1)$$

$$\frac{\partial}{\partial t}W^*(x,t) = D^*\frac{\partial^2}{\partial x^2}W^*(x,t) - \gamma^* W^*(x,t) + [kGW(x,t) - k'W^*(x,t)] - [k_{Rg} RW^*(x,t) - k_{Rg}' R_g^*(x,t)] \quad (2)$$

$$\frac{\partial}{\partial t}R^*(x,t) = k_R RW(x,t) - k_R' R^*(x,t) - \alpha^* R^*(x,t) \quad (3)$$

$$\frac{\partial}{\partial t}R_g^*(x,t) = k_{Rg} RW^*(x,t) - k_{Rg}' R_g^*(x,t) - \alpha^* R_g^*(x,t) \quad (4)$$

$$\frac{\partial}{\partial t}R(x,t) = -k_{Rg} RW^*(x,t) - k_R RW(x,t) + k_{Rg}' R_g^*(x,t) + k_R' R^*(x,t) - \alpha R(x,t) + \Gamma(x) \quad (5)$$

where W and W^* are, respectively, the areal densities of free and glypican-bound morphogen on the surface, whereas G and R are free glypican and receptor areal densities.

To simplify presentation, we reduced the description of free morphogen diffusion (Eq. (1)) to two dimensions (i.e., along cell surface). This is the case explicitly whenever morphogen diffusion occurs in a narrow intercellular space between juxtaposed cell surfaces. Furthermore, in Appendix B we show that even in the case of morphogen on and near an exposed cell surface, the analysis of full three-dimensional diffusion, under the conditions of relatively rapid degradation of free extracellular morphogen, also reduces to Eq. (1). As an additional simplification, we shall only consider variation along the direction, x, perpendicular to the line source of morphogen. The $s\delta(x)$ term on the right-hand side of Eq. (1) represents the source of morphogen along the line with coordinate $x=0$, representing the locus of morphogen secreting cells corresponding to the compartment boundary.

In addition to diffusion of free morphogen W and its degradation (or loss off the surface) with rate γ, Eq. (1) describes morphogen W binding to glypican G and receptor R. W, W^*, R and R^* vary in time t and space x. Eq. (2) describes surface diffusion of W^*, its degradation with rate γ^*, conversion of between free and glypican-bound moieties and reversible binding of W^* to R forming the receptor-morphogen–glypican complex R_g^*. Eqs. (3)–(5) describe receptor-morphogen binding. For complete generality, we allow receptor activation by free, W, or glypican-bound, W^*, morphogen. Although in the first case glypicans compete with receptors for morphogen, in the latter case glypican acts as a co-receptor that "presents" the morphogen molecule to the receptor. The kinetics

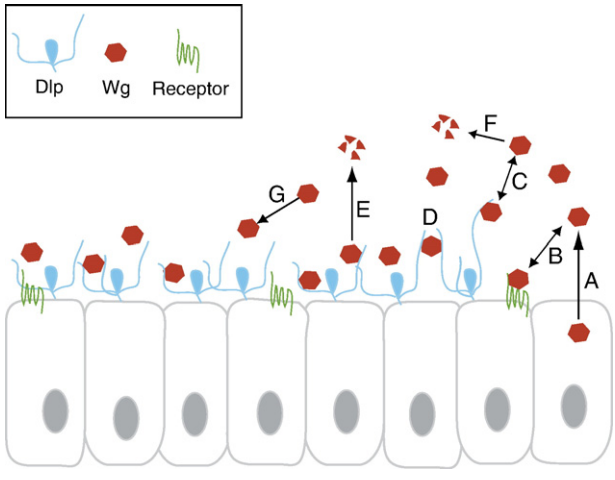

Fig. 3. Cartoon representing the process of morphogen spreading. (A) Morphogen (red) secretion by source cells; (B) binding of morphogen to receptors (green); (C) binding of morphogen to surface glypicans (cyan); (D) morphogen diffusion in the glypican layer; (E) degradation of the morphogen–glypican complex by shedding or destruction after internalization; (F) degradation of free morphogen; (G) free morphogen diffusion.

of receptor binding to W and W^* is parameterized in Eqs. (3)–(5) by k_R, k'_R and k_{Rg}, k'_{Rg}.

In modeling the dynamics of the morphogen receptor (Eqs. (3)–(5)) in addition to ligand binding reactions, we have introduced the effect of receptor endocytosis (Seto and Bellen, 2004; Strigini and Cohen, 2000) parameterized by two rates α and α^*, respectively, governing the uptake of free and ligand-bound receptors. Receptor density is maintained by continuous production of the receptor protein parameterized by Γ on the right-hand side of Eq. (5).

In addition to spatially varying W, W^*, R, R^* and R^*_g densities, Eqs. (1)–(5) allow spatial variation of key parameters, such as the total glypican density $G_{\mathrm{tot}}=G+W^*$ and the rate of receptor production Γ. The dependence of the latter on position reflects feedback regulation of glypicans and receptors by morphogens and other signals (Crickmore and Mann, 2006; Han et al., 2005). Another parameter likely to present spatial modulation is the W^* degradation rate γ^*. It is expected that in all of these cases spatial modulation of parameters controlling morphogen propagation and transduction is the result of morphogen signaling and therefore is a feedback effect. One example of such a feedback for the case of Wg morphogen is provided by recent findings of (Giraldez et al., 2002) and (Kreuger et al., 2004). These studies have demonstrated that Notum - an enzyme induced by high Wg levels near the DV boundary - induces cleavage of Dlp glypican at the level of its GPI anchor. The cleavage of Dlp would also release Wg–Dlp complexes from the surface which is exactly the process that we model via γ^* term in Eq. (2). Notum is also known to act via Dally (Han et al., 2005), which would within our approximations lead to a similar phenomenological term in the model.

The model is stated here in a rather general form, which can be further generalized by introducing several glypican species (see Appendix C) interacting with the same morphogen. For example, Wg in *Drosophila* wing discs interacts with both Dlp and Dally. We shall argue that quite generally the model can be reduced to a single "effective" glypican specie whose properties represent the combined effect of the components.

Results

The model described by Eqs. (1)–(5) is analyzed in Appendix A where we show that glypican-bound moiety, W^*, dominates transport in the regime where degradation (or loss) of the free moiety in is faster than rate of glypican/morphogen complex dissociation (so that $\gamma > k'\ D/D^*$ is satisfied). Glypicans are important to the extent that the glypican-bound morphogen is protected from degradation enough to make the diffusion length of the W^* complex *on* the cell surface longer than the diffusion length of free moiety, W, *off* the surface: $\sqrt{D^*/k'} > \sqrt{D/\gamma}$. As a result, the spreading of morphogen becomes dependent on glypican concentration.

To understand the mechanism underlying the dependence of morphogen signaling on glypican concentration, we will first describe the behavior of the model with several simplifying assumptions: (a) constant glypican density; (b) morphogen–glypican binding far from saturation (i.e., $G >> W^*$); (c) degradation of morphogen–glypican complex negligible compared to the rate of degradation of free morphogen. Note that in the steady state the effect of receptor endocytosis boils down to an increased rate of morphogen degradation and thus in the present discussion is subsumed within γ and γ^*. One finds (see Appendix A) that in the steady state glypican-bound morphogen profile behaves as (see Fig. 4A)

$$W^*(x) \sim \frac{g}{\sqrt{1+g}} e^{-x/\lambda} \tag{6}$$

with dimensionless glypican density, $g=kG/\gamma$ and the length scale λ given by

$$\lambda^2 = (1+g)\frac{D^*}{k'} \tag{7}$$

Length scale λ sets the range of morphogen spreading. We observe that this range increases with increasing glypican

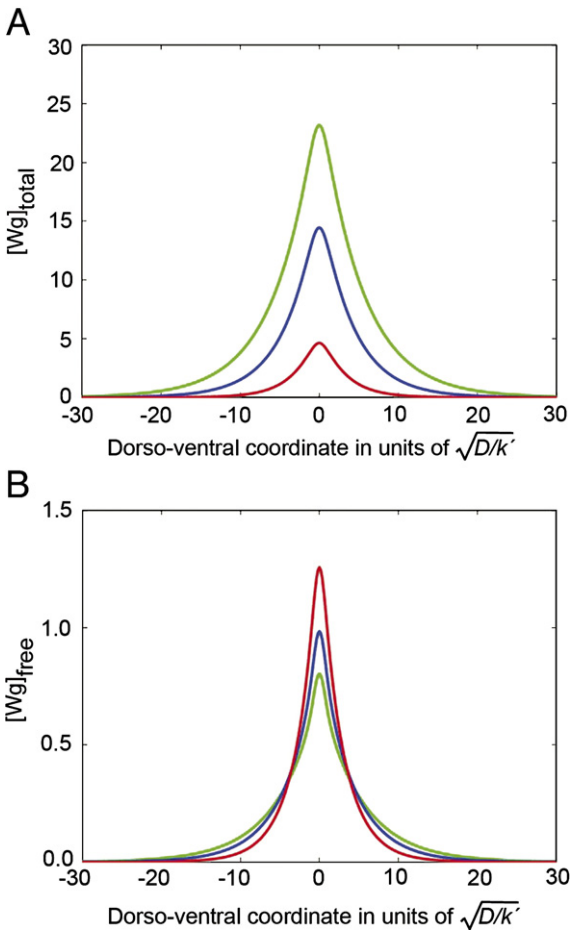

Fig. 4. Predicted effects of glypican surface density on (A) total Wg level and (B) the level of free Wg with signaling capacity. Result of a numerical solution of Eqs. (1)–(5) with the generic morphogen, W, identified as Wg. Glypican (Dlp) levels with g=10, 50 and 100 are indicated by the red, blue and green lines, respectively. (A) An increase in Dlp levels (red to green) leads to an increase of total Wg, which is dominated by the surface-bound moiety. (B) The concentration of free Wg at the surface is reduced by increased levels of Dlp at the DV boundary, but increased further away from the DV boundary, where Wg levels are normally low.

density, which happens because binding to glypican "protects" the morphogen from being lost but still allows diffusion along the surface. Thus, Eqs. (6) and (7) tell us that an increase in G and therefore in g, by decreasing the rate of exponential decay with distance, causes an increase in $W^*(x)$ at positions far from the source. We see also that close to the source of morphogen (at $x=0$), $W^*(0)$ increases as well (see Fig. 4A). Free morphogen concentration is, on the other hand, approximately given by

$$W(x) = \frac{k'}{g\gamma} W^*(x) \sim \frac{e^{-x/\lambda}}{\sqrt{1+g}} \tag{8}$$

which implies that the free morphogen concentration in the region close to the source behaves as a function of g in the way opposite to W^* (see Fig. 4B). Thus, whereas free morphogen concentration at the surface sufficiently far from the source is enhanced by increasing G (and hence g) because of the increased range of spreading, close to the source (where the exponential in Eq. (8) is close to unity) *free* morphogen concentration is suppressed by the increased recruitment into the glypican complex.

The reduction of free morphogen near DV boundary provides a possible explanation for the observed suppression of Wg signal by Dlp overexpression. Let us for the simplicity of presentation for a moment neglect receptor endocytosis. Then in a steady state, the receptor is in equilibrium with local concentrations of W and W^* (and therefore does not affect their spatial distribution) which implies that

$$R^* + R_g^* = R_{tot} \frac{K_R^{-1} W + K_{Rg}^{-1} W^*}{1 + K_R^{-1} W + K_{Rg}^{-1} W^*} \tag{9}$$

where $K_R = k'_R / k_R$ and $K_{Rg} = k'_{Rg} / k_{Rg}$ are the equilibrium constants for receptor binding to W and W^*, respectively. If receptor binds free morphogen much more strongly than its glypican-bound moiety, $K_{Rg}/K_R >> W^*/W \sim g$, free morphogen dominates signaling. In this case, sequestration and therefore suppression of free morphogen by glypican overexpression predicted by the model (Eq. (8)) would result in the suppression of signal near DV boundary. We therefore propose this is indeed the case for Wg, Dlp and Fz2 receptors in wing disc.

The functional dependence on glypican concentration described above is independent of parameters as long as the surface diffusion length is longer than the diffusion length in the intercellular space as stated above (which requires $\gamma / k' > D/D^*$). The generality of this dependence is reassuring because actual values of parameters are at present not known. We know, however, that parameters are such that the morphogen spreading length scale λ is about 10 μm (which may be compared to the dorso-ventral dimension of the wing pouch, about 150 μm). If we assume plausible values for D, D^*, binding affinity $k'/k \sim 1$ μM and $k' \sim 1\ s^{-1}$ (Kreuger et al., 2003) as summarized in Appendix D, we can restate this constraint as an estimate of glypican concentration (derived from Eq. (7)) which comes out to be $G > 5 \times 10^6$/cell—consistent with the expected (high) level of HSPG expression. It should be noted that strictly speaking, G, refers to the density of morphogen *binding sites* on the surface, so if each glypican (i.e., its HS chains) holds several binding sites, the concentration of the glypican itself can be lower.

With the simplifying assumptions stated at the beginning of this section, the model predicts simple exponential profiles for both W and W^* concentrations away from the source. The observed Wg distribution profiles (Figs. 2A and 5), however, are not well approximated by exponentials. Wg profiles are steeper close to the DV boundary than they are in the peripheral regions. Two effects could act to modify the spatial profile of morphogen close to its source. The first is the reduced Dlp density near DV boundary observed in winged discs (Han et al., 2005). The second is the higher rate of degradation of glypican-bound morphogen (W^*) close to morphogen source, where its concentration is higher. This effect is conjectured on the basis of the observed activity of Notum in clipping Dlp (Giraldez et al., 2002) and Dally (Han et al., 2005). Both effects should be regarded as manifestations of negative feedback because both the expression of Notum and repression of Dlp near DV boundary are consequences of the high level of transduced Wg signal.

It is relatively straight-forward to analyze our model with spatially modulated glypican density; however, as we shall see below, the effect of Wg dependent degradation alone can already account for the observed Wg profiles. Thus, for the sole reason of reducing the number of free parameters in the model we will continue to hold glypican density constant. This constraint can be relaxed once new quantitative data on glypican (and Wg) distribution in imaginal discs warrants a model with more parameters. Furthermore, we expect low density of Dlp near DV boundary to be partially compensated by the abundance of Dally (see Discussion section).

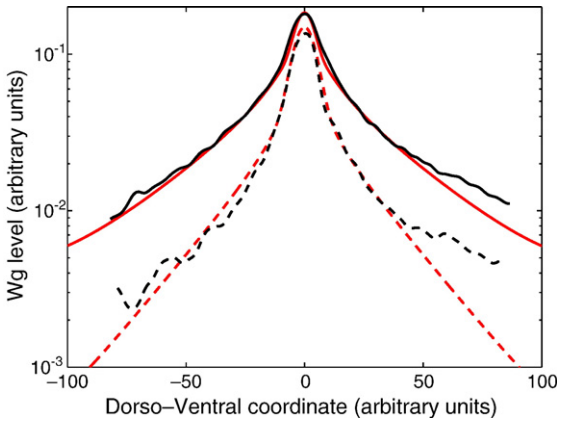

Fig. 5. Comparison of the observed Wg profiles with morphogen profiles computed for the model including morphogen signal dependent degradation of morphogen–glypican complex. Dashed and solid black lines are, respectively, Wg profiles measured in the anterior and posterior regions of an enGal4>Dlp disc. Note semi-log scale, which makes explicit the deviation from a simple exponential profile, which would appear as a straight line. Red lines represent numerical fits according to Eqs. (1)–(5) with a negative feedback term (Eq. (10)) representing the action of Notum enzyme. The numerical fits in anterior and posterior compartment differ only in their Dlp levels (g=475 anterior, g=1050 posterior). The increase of the Dlp level in the posterior compartment leads to an increase in total Wg level. Note that the model reproduces the changes in the tails of the Wg profiles as well as the increase in the central region.

Let us consider the effect of enhanced degradation of W^* complex in the region of high morphogen signal. To incorporate such an effect we make degradation rate of the W^* complex, i.e., γ^* in Eq. (2), explicitly depend on receptor activation, which as shown above (Eq. (8)) is explicitly related to W and W^*. For simplicity, we assume that signaling is dominated by W (although this assumption is not essential) and parameterize $\gamma^*(W)$ by a sigmoidal function:

$$\gamma^*(W) = \gamma_0^* + \gamma_m^* \frac{W^n}{w_0^n + W^n} \quad (10)$$

with the maximal rate γ_m^*, Hill constant n and a characteristic morphogen concentration w_0. Clearly, non-linear degradation contributes only in the range $1 > W/w_0 > (\gamma_0^*/\gamma_m^*)^{1/n}$ where the second term of Eq. (9) dominates over the first. In that intermediate range, the problem relates closely to the model of non-linear degradation of diffusible messenger molecule studied by Eldar et al. (2003). Analysis of the model (Eqs. (1)–(4)) including the feedback effect due to $\gamma^*(W)$ proceeds via a numerical solution of the steady state equations (see Appendix A) as described in the Materials and methods section. Comparing the results of the numerical simulation of the model with the measured Wg profiles (see Fig. 5) allows us to estimate effective parameters for W dependent W^* degradation (i.e., parameters in Eq. (9)). These parameter values are quoted in Appendix D. We can also compare fits of Wg profiles in the anterior and posterior domains of the *en*Gal4 > Dlp which differ only in the concentration of the Dlp. We find that Wg levels in the posterior compartment can be fit by the model with glypican density G about twice as high as the WT glypican density in the anterior compartment.

Discussion

Our results suggest a simple explanation for the observed opposite effects of Dlp on Wg signal near and far from the DV boundary (Kreuger et al., 2004). To make contact between our analysis and the experiments, we interpret measurements of Wg distribution in the imaginal disc (Figs. 1 and 2A, C) as the measurement of total Wg at the surface, which is dominated by the density of surface-bound Wg moiety (i.e., W^*). Like W^* in the model, observed Wg is enhanced throughout the posterior compartment where Dlp is overexpressed. However, the effect on Wg signaling as evidenced by the level of expression of the "high threshold" downstream target Sens and the "intermediate threshold" target Dll, shown in Figs. 2C, D, is suppressed close to the Wg source at the DV boundary. The reduction of Wg signal near the DV boundary and the enhancement of Wg signal far from the boundary would follow from our analysis, provided that the active signaling moiety of Wg is the free moiety at the cell surface. Thus, we conclude that instead of acting as co-receptor (Lin and Perrimon, 1999), Dlp glypican is actually competing with Wg receptor for the ligand.

The observed deviation of Wg distribution profiles from exponentials can be accounted for by introducing a negative feedback that enhances morphogen–glypican degradation, where Wg signal is strong. The former effect represents in a simplified form the effect of Notum enzyme, which is expressed in the high Wg signal region near the DV boundary (Giraldez et al., 2002; Han et al., 2005). Mathematically, signal-dependent degradation of the glypican-bound morphogen moiety in our model closely approximates non-linear degradation considered by Eldar et al. (2003).

A number of recent studies (Crickmore and Mann, 2006; Marois et al., 2006; Rives et al., 2006; Seto and Bellen, 2006) report the important role of receptor mediated endocytosis in shaping morphogen gradients. As far as the latter is concerned, receptor endocytosis is parameterized by morphogen degradation rates. It does, however, allow a very interesting mode of regulation and adaptation to morphogen signal. A particularly intriguing possibility is illustrated by the following observation. Let us consider the total receptor density in a steady state. The condition for a steady state of the total receptor density is found by adding Eqs. (4)–(6) together and setting the left-hand side to zero. Lets us for a moment assume that only the ligand-bound form of the receptor undergoes endocytosis so that $\alpha = 0$. It then follows that in a steady state the total ligand-bound receptor density is given by $R^* + R_g^* = \Gamma/\alpha^*$, which is completely independent of ligand concentration! This striking result is an example of "perfect adaptation" (Barkai and Leibler, 1997) known to engineers as integral feedback (Goodwin et al., 2001). It happens here because lower level of the ligand is exactly compensated by the accumulation of free receptors (produced at constant rate), whereas high level of the ligand means high rate of receptor uptake resulting in low receptor density. In the regime of *perfect* adaptation all dependence of R^* on morphogen level would be transient and it is therefore not a plausible regime for morphogen signaling in the imaginal disc. However, the regime where free receptor recycles at a significantly slower rate than the ligand-bound receptor, $\alpha << \alpha^*$ is quite possible. In this regime R^* will depend on W level although the steady state response will be attenuated by the adaptation of total receptor density. This is an interesting possibility to have in mind because it could account for some of the observed modulation of receptor density.

It is interesting to compare, in the context of our model, the observed effects of Dlp and Dally on Wg signaling (Han et al., 2005). The model is intended to apply equally well to either glypican and is readily extended (see Appendix C) to describe both. It is, however, expected that Dlp and Dally interaction with Wg is quantitatively different. Experiments of Han *et al*. (Han et al., 2005) reveal an enhancement of Wg by overexpression of Dally although somewhat weaker than in the case of Dlp. In contrast to the case of Dlp, overexpression of Dally facilitates Wg signaling near DV boundary. These observations can be understood in term of our model provided that (a) effective diffusion length of the Wg-Dally complex is smaller than that for Wg-Dlp, and (b) unlike Wg-Dlp, Wg-Dally complex binds effectively to Wg receptors. In quantitative terms condition (a) corresponds to $D^*_{Dally}[Dally]/K_{Dally} < D^*_{Dlp}[Dlp]/K_{Dlp}$ (where K_{Dally} and K_{Dlp} equilibrium constants for Wg binding, respectively to Dally and Dlp). Assuming surface densities of Dally and Dlp are comparable, this suggests that Wg affinity for Dally

is lower than that for Dlp and/or that Wg-Dally diffusivity is smaller than that of Wg-Dlp. Condition (b) implies $K_{R,\mathrm{Dally}}/K_R < g_{\mathrm{Dally}}$, which contrasts $K_{R,\mathrm{Dlp}}/K_R >> g_{\mathrm{Dlp}}$. (where $K_{R,Dally}$ and $K_{R,Dlp}$ are equilibrium constants for receptor binding Wg-Dally and Wg-Dlp complexes, whereas K_R is the equilibrium constant for receptor binding free Wg.) Thus using the model to interpret experimental observations suggests that Dally but not Dlp acts as a "co-receptor" of Wg. This conclusion is consistent with the recent results of Franch-Marro et al. (2005). Another phenomenon differentiating the effects of Dlp and Dally is their interaction with Notum, which appears to be more effective at cleaving Dlp than Dally. The model described here can readily describe the effect of variation of density of different glypicans throughout the disc. In fact we know that Dlp density is depressed near DV boundary (Han et al., 2005; Kirkpatrick et al., 2004; Kreuger et al., 2004). As a result, in that region of WT disc one may expect Dally to be the dominant component of glypican density. Yet, Dlp plays a role near the boundary to reduce (free) Wg levels because its removal leads to elevated Wg signaling (Giraldez et al., 2002). In Appendix C, we show that morphogen spreading in the presence of multiple glypican species behaves as if there was but a single "effective" glypican density with properties such as affinity for morphogen (or the diffusivity and the degradation rate of the morphogen–glypican complex) determined by the properties and relative abundance of its components. Because of the variation in the relative abundance of Dally and Dlp, we expect the properties of the "effective" glypican (describing the combined effect of Dlp and Dally) to vary with distance from the DV boundary, being closer to the properties of Dally near DV boundary and closer to Dlp away from the boundary. At present there is not enough quantitative data to attempt fitting the observations with a model with spatially variable parameters. On the other hand, our analysis and the ability to approximately fit the data by the model with constant parameters suggest that the latter provides a good starting point for further elaboration in the future.

An essential ingredient of the mechanism described above rests on the assumption that glypican-bound morphogen retains mobility along cell surface[2]. An interesting possible mechanism for such mobility would require morphogen to have multiple binding sites for HS arms of glypicans. This would allow "brachiation": i.e., morphogen molecule changing glypican "partners" while still being bound within the glypican layer (Levin et al., 2002).

In addition to explaining (and fitting) observations, the present model makes a number of quantitative predictions. For example, by comparing Wg profiles in the anterior and posterior compartments of discs overexpressing Dlp in the posterior compartment, we can use the model to estimate the ratio of Dlp levels in the two compartments. This estimate can then be tested with a direct measurement (of the ratio) of Dlp levels in the two compartments provided Wg and Dlp were measured by immuno-fluorescence on the same disc. The model also predicts quantitatively the non-autonomous effect that overexpression of Dlp in, say, dorsal compartment would have on Wg level in the ventral compartment: the latter would be increased. It also predicts the effect that over- or under-expression of Notum would have on Wg profile (see Fig. 6). Thus, modeling serves to (a) explain non-trivial phenotypes; (b) extract more information and understanding from the data by quantitative analysis; and (c) generate predictions, which make models falsifiable and provide interesting and non-trivial hypotheses to guide future experiments.

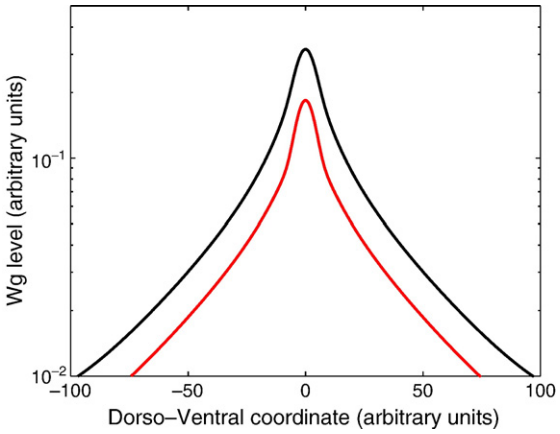

Fig. 6. Predicted effect of Notum overexpression on the shape of Wg distribution. Doubling the level of Notum (represented by doubling γ_m^*) in the model is predicted to lead to a sharper Wg peak at the DV boundary and a lower over-all Wg level (red) compared to the wild type (black).

Materials and methods

Fly strains

en-Gal4 is described in Flybase. UAS-Dlp-HA is a modification from (Baeg et al., 2004) Baeg et al. (2001), described in Giraldez et al. (2002).

Antibodies

Rat anti-Dll was produced by Jun Wu, mouse anti-Senseless was a gift from Dr. H.J. Bellen (Nolo et al., 2000), overexpressed Dlp-HA was detected with rat anti-HA (Roche). The Wg antibody was produced as described (Brook and Cohen, 1996).

Data collection

Confocal images of antibody staining of the wing imaginal discs used in the present study to quantify Wg distribution profiles are projections of four image sections taken at different depths of the wing discs. The projections reflect protein levels in the full disc space.

Numerical methods

The steady state solution of Eqs. (1–4) was found by discretizing the Laplacian and using the Newton–Raphson iteration scheme to find the roots of the corresponding system of non-linear equations. The solution of the linear part of equations served as a starting point for the iteration.

[2] A model of morphogen/glypican interaction was proposed and simulated numerically in a recent paper by Cinquin (Cinquin (2006). Fast-tracking morphogen diffusion. J Theor Biol 238, 532–40). This model considers equilibration between glypican-bound and free morphogen species but does not allow for diffusion of the morphogen–glypican complex. This model does not explain the effects of glypican overexpression discussed above.

Acknowledgments

LH was supported in part by a Fellowship of the Max Planck Society. JK was supported by the Wenner-Gren foundation. BIS acknowledges support from the NIH grant GM67794.

Appendix A. Detailed solution of the model

Let us solve for the steady state of Eqs. (1)–(5).

$$D\frac{\partial^2}{\partial x^2}W(x) - \gamma W(x) - [kGW(x) - k'W^*(x)] - \alpha^* R^* + s\delta(x) = 0 \quad (\mathrm{AI}-1)$$

$$D^*\frac{\partial^2}{\partial x^2}W^*(x) - \gamma^* W^*(x) + [kGW(x) - k'W^*(x)] - \alpha^* R_g^* = 0 \quad (\mathrm{AI}-2)$$

$$k_R RW(x,t) - k_R' R^*(x,t) = \alpha^* R^*(x,t) \quad (\mathrm{AI}-3)$$

$$k_{Rg} RW^*(x,t) - k_{Rg}' R_g^*(x,t) = \alpha^* R_g^*(x,t) \quad (\mathrm{AI}-4)$$

$$k_{Rg} RW^*(x,t) + k_R RW(x,t) - k_{Rg}' R_g^*(x,t) - k_R' R^*(x,t) = \Gamma - \alpha R(x,t) \quad (\mathrm{AI}-5)$$

In a steady state, receptor equilibration with W and W^* is offset by endocytosis which is represented by the α^* dependent term on the right-hand side of Eqs. (AI-3) and (A1-4) and in Eqs. (AI-1) and (AI-2). By solving Eqs. (AI-3), (AI-4), and (AI-5) Eqs. (AI-1) and (AI-2) can be approximately by degradation terms. Let us illustrate this in a simplified form on the basis of Eqs. (AI-1), (AI-3), and (AI-4)where we shall set $W^*=0$. In that case, Eqs. (AI-3) and (A1-4) can be reduced to $\alpha R + \alpha^* R^*(x,t) = \Gamma$ and $k_R RW = (k_R' + \alpha^*)R^*$ which together yield

$$\alpha^* R^* = k_R W \frac{\alpha^* \Gamma}{\alpha(k_R' + \alpha^*) + \alpha^* k_g W} \quad (\mathrm{AI}-6)$$

When substituted into Eq. (AI-1) this term looks like a degradation term that saturates at high W but at low W it simply adds to the linear degradation term γ.

Assuming that glypican concentration is sufficiently high that saturation effects can be neglected makes Eqs. (AI-1) and (AI-2) linear. If, in addition, G is assumed to be constant, the steady state solution is readily found in terms of a Fourier transform with respect to surface coordinates: $W^*(x) \to w_q^*$ and $W(x) \to w_q$. Because we are interested in a situation with a line source of morphogen we need to consider only surface coordinate x perpendicular to the source (i.e., DV boundary in the case of Wg).

$$[\gamma + kG + Dq^2]w_q = k'w_q^* + s \quad (\mathrm{AI}-7)$$

$$[\gamma^* + k' + D^*q^2]w_q^* = kGw_q \quad (\mathrm{AI}-8)$$

Substituting w_q determined from Eq. (AI-8) into Eq. (AI-7) one arrives for the expression relating w_q^* with the rate of morphogen secretion by the line source, s:

$$[\gamma + kG + Dq^2][\gamma^* + k' + D^*q^2]w_q^* = kG(k'w_q^* + s) \quad (\mathrm{AI}-9)$$

and defining $g = kG/\gamma$ we obtain

$$\left\{k' + (1+g)\gamma^* + \left[\frac{\gamma^* + k'}{\gamma}D + (1+g)D^*\right]q^2 + \frac{DD^*}{\gamma}q^4\right\}W_q^* = gs \quad (\mathrm{AI}-10)$$

The q^4 term is important only at short distance, i.e., very close to the source, so that the solution is approximated by

$$w_q^* = \frac{gs}{\Gamma}\frac{1}{1+\lambda^2 q^2} \quad (\mathrm{AI}-11)$$

where $\Gamma = k' + (1+g)\gamma^*$ and $\lambda^2 = \frac{(1+g)D^* + \gamma^{-1}(\gamma^* + k')D}{\Gamma}$. The glypican-bound morphogen moiety dominates morphogen spreading if $(1+g)D^* >> \gamma^{-1}(\gamma^* + k')D$ and morphogen spreading is enhanced by glypican concentration if glypican-bound morphogen is degraded sufficiently slowly: $(1+g)\gamma^* << k'$. Under these conditions, the expression for the characteristic length of morphogen transport reduces to $\lambda^2 = \frac{(1+g)D^*}{k'}$ quoted in the Results section. Fourier transform back to x-space yields Eq. (7).

Appendix B. Derivation of the model of morphogen spreading on the surface

Let us derive Eqs. (1) and (2) describing morphogen spreading along the surface for the more general case where morphogen W is free to diffuse in three dimensions in the *extracellular* space bounded on one side by cell surface, while reversibly binding glypicans and receptors on the cell surface. Diffusion and degradation in the extracellular space are described by

$$\frac{\partial}{\partial t}W(x,y,z,t) = D\nabla^2 W(x,y,z,t) - \gamma_0 W(x,y,z,t) \quad (\mathrm{AII}-1)$$

where D is diffusivity of free morphogen and γ_0 is the rate of its degradation in extracellular space. Coordinate z measures distance to cell surface. To simplify presentation, we shall ignore the possibility of variation along one of the surface axis and drop the y coordinate. Morphogen secretion along with the interaction with surface glypican, G, and morphogen receptor, R, is described by

$$D\frac{\partial}{\partial z}W(x,z,t)|_{z=0} = -s\delta(x) + [k_0 GW(x,0,t) - k'W^*(x,t)] + [k_{0R}RW(x,0,t) - k_R' R^*(x,t)] \quad (\mathrm{AII}-2)$$

where $W(x,0,t)$ is the three-dimensional concentration at the surface, $z=0$. Left-hand side is the flux of W onto (or off) the surface. The 1st term on the right-hand side represents a line source of morphogen on the surface (along $x=0$) and the terms in square brackets describe reversible formation of morphogen/glypican complex W^* and reversible binding to the receptor: $W+R \leftrightarrow R^*$. Eq. (AII-2) specifies the $z=0$ boundary condition for Eq. (AII-1). The second boundary condition is $W \to 0$ for $z \to \infty$.The dynamics of the glypican-bound morphogen on cell surface is described by

$$\frac{\partial}{\partial t} W^*(x,t) = D^* \frac{\partial^2}{\partial x^2} W^*(x,t) - \gamma^* W^*(x,t) + \left[k_0 G W(x,0,t) - k' W^*(x,t)\right] - \left[k_{Rg} R W^*(x,t) - k'_{Rg} R^*_g(x,t)\right] \quad (\text{AII}-3)$$

where D^* and γ^* are its diffusivity and the degradation rate. $W_0=W(x,0,t)$ is the concentration of free morphogen at the surface. Receptor activation is governed by Eqs. (3) and (4).

We proceed by solving Eq (AII-1) subject to the boundary condition Eq. (AII-2) at the surface and $W \to 0$ as $z \to \infty$. Fourier transforming Eq (AII-1) with respect to time and surface coordinates,[3] $W_{q,\omega}(z)=\int dx e^{iqx} \int \mathrm{d}t e^{i\omega t} W(x,z,t)$ one finds that free morphogen concentration decays exponentially away from the surface as

$$W_{q,\omega}(z) = u_q e^{-\frac{z}{\sqrt{D}}\sqrt{\gamma + i\omega + Dq^2}} \quad (\text{AII}-4)$$

with

$$\sqrt{D}\sqrt{\gamma + i\omega + Dq^2} u_q = F_{q,\omega} \quad (\text{AII}-5)$$

the right-hand side of which is the Fourier transform of the right-hand side of Eq. (AII-2) with respect to t and x. To the extent that we are interested in the behavior at long times and distances and assume that morphogen degradation in extracellular space is rapid, we can assume $i\omega,\ Dq^2 \ll \gamma_0$ and approximate the square root on the left-hand side of Eq. AII-5 as

$$D^{1/2}\sqrt{\gamma_0 + i\omega + Dq^2} \approx (i\omega + Dq^2 + 2\gamma_0)(D/4\gamma_0)^{1/2} \quad (\text{AII}-6)$$

Substituting into Eq. (AII-5), Fourier transforming back to (x,t) coordinates, and identifying $W_S(x,t)=(D/4\gamma_0)^{1/2} W(x,0,t)$ as the effective *area density* of free morphogen at the surface, we recover Eq. (1) as the equation governing dynamics of W_S:

$$\frac{\partial}{\partial t} W_S(x) = \frac{D}{2} \nabla^2 W_S(x) - \gamma(1+g) W_S(x) + k' W^*(x) + k'_R R^*(x) + S\delta(x) \quad (\text{AII}-7)$$

with parameters $\gamma=2\gamma_0$ and $k=k_0(D/4\gamma)^{-1/2}$ as well as $k_R=k_{0R}(D/4\gamma_0)^{-1/2}$ determined in terms of the kinetic constants of the underlying three-dimensional processes. Note that g - the dimensionless measure of glypican density - was defined as $g=G/G_0$ with $G_0=\sqrt{D\gamma}/k$. Thus, we have derived an effective model describing two-dimensional spreading of free and glypican-bound moieties on the surface that provided us with the departure point for our analysis. This reduction of the three-dimensional model (without great loss of accuracy in the regime of interest) to two dimensions is particularly useful for the purpose of numerical simulation, which becomes necessary when we analyze the effect of the morphogen dependent W^* degradation.

Appendix C. Generalization of the model to multiple glypican species

Eqs. (1)–(4) and their derivation can be readily generalized to include binding of morphogen to multiple glypican species with concentrations G_i.

$$\frac{\partial}{\partial t} W = D \frac{\partial^2}{\partial x^2} W - \gamma W - \sum_i \left[k_i G_i W - k'_i W^*_i\right] - \left[k_R R W - k'_R R^*\right] + s\delta(x) \quad (\text{AIII}-1)$$

$$\frac{\partial}{\partial t} W^*_i = D^*_i \frac{\partial^2}{\partial x^2} W^*_i - \gamma^*_i W^*_i + \left[k_i G_i W - k'_i W^*_i\right] - \left[k_{Rg,i} R W^*_i - k'_{Rg,i} R^*_{g,i}(x)\right] \quad (\text{AIII}-2)$$

where W^*_i denotes areal density of morphogen bound to glypican "i", and all parameters with "i"-subscript refer to the corresponding glypican specie. One can show that Eqs. (AIII-1) and (AIII-2) can be approximately reduced to an "effective" model, in the form of Eqs. (1) and (2), with different glypican species described collectively as a single "effective glypican", G_{eff}, with areal density given by a weighted average of different glypican species: $G_{eff} = \frac{1}{k_{eff}} \sum_i k_i G_i$ and $k_{eff} = \sum_i k_i$. For the steady state this effective model reduces to

$$D \frac{\partial^2}{\partial x^2} W - \gamma W - \left[k_{eff} G_{eff} W - k'_{eff} W^*_{eff}\right] + s\delta(x) = 0 \quad (\text{AIII}-3)$$

$$D^*_{eff} \frac{\partial^2}{\partial x^2} W^*_{eff} - \gamma^*_{eff} W^*_{eff} + \left[k_{eff} G_{eff} W - k'_{eff} W^*_{eff}\right] = 0 \quad (\text{AIII}-4)$$

with $W^*_{eff} = \frac{1}{k'_{eff}} \sum_i k'_i W^*_i$ describing glypican-bound morphogen and other effective parameters defined as: $k'_{eff} = \sum_i k'_i$, $\gamma^*_{eff} = \frac{1}{k_{eff} G_{eff}} \sum_i k_i G_i \gamma^*_i$, and $D^*_{eff} = \frac{1}{k_{eff} G_{eff}} \sum_i k_i G_i D^*_i$. These reduced equations provide a good approximation provided spatial variation is slow and γ^*_i is small compared to k'_i.

Appendix D. Summary of estimated parameters of morphogen–glypican interaction

Parameters describing morphogen diffusivity, rate of degradation and interaction with glypicans are not known at present. Here we make some order of magnitude guesses, guided by the consistency with the observed length scale of Wg spreading

[3] Because we are interested in a situation with a line source of morphogen, we need to consider only surface coordinate x perpendicular to the source (i.e., DV boundary in the case of Wg).

($\lambda \sim 10$ μm) and the condition, $\sqrt{D^*/k'} > \sqrt{D/\gamma}$, of surface diffusion dominance.

D	10 $\mu m^2/s$
D^*	>1 $\mu m^2/s$
γ	>10 s^{-1}
k'/k	1 μM (Kreuger et al., 2003)
k'	>1 s^{-1} (Kreuger, unpublished)
G	6×10^6/cell
a (cell size)	3 μm
γ^*	1 s^{-1}
w_0	$s\sigma\sqrt{D\gamma}$ with $\sigma=66$
n	2
s	Arbitrary scale

In setting parameters for numerical simulations, we replaced inequalities by equalities.

References

Baeg, G.H., Lin, X., Khare, N., Baumgartner, S., Perrimon, N., 2001. Heparan sulfate proteoglycans are critical for the organization of the extracellular distribution of Wingless. Development 128 (1), 87–94.

Baeg, G.H., Selva, E.M., Goodman, R.M., Dasgupta, R., Perrimon, N., 2004. The Wingless morphogen gradient is established by the cooperative action of Frizzled and Heparan Sulfate Proteoglycan receptors. Dev. Biol. 276, 89–100.

Barkai, N., Leibler, S., 1997. Robustness in simple biochemical networks. Nature 387, 913–917.

Belenkaya, T.Y., Han, C., Yan, D., Opoka, R.J., Khodoun, M., Liu, H., Lin, X., 2004. *Drosophila* Dpp morphogen movement is independent of dynamin-mediated endocytosis but regulated by the glypican members of heparan sulfate proteoglycans. Cell 119, 231–244.

Bernfield, M., Kokenyesi, R., Kato, M., Hinkes, M.T., Spring, J., Gallo, R.L., Lose, E.J., 1992. Biology of the syndecans: a family of transmembrane heparan sulfate proteoglycans. Annu. Rev. Cell Biol. 8, 365–393.

Bernfield, M., Gotte, M., Park, P.W., Reizes, O., Fitzgerald, M.L., Lincecum, J., Zako, M., 1999. Functions of cell surface heparan sulfate proteoglycans. Annu. Rev. Biochem. 68, 729–777.

Brook, W.J., Cohen, S.M., 1996. Antagonistic interactions between wingless and decapentaplegic responsible for dorsal–ventral pattern in the *Drosophila* leg. Science 273, 1373–1377.

Cinquin, O., 2006. Fast-tracking morphogen diffusion. J. Theor. Biol. 238, 532–540.

Crickmore, M.A., Mann, R.S., 2006. Hox control of organ size by regulation of morphogen production and mobility. Science 313, 63–68.

Eldar, A., Barkai, N., 2005. Interpreting clone-mediated perturbations of morphogen profiles. Dev. Biol. 278, 203–207.

Eldar, A., Dorfman, R., Weiss, D., Ashe, H., Shilo, B.Z., Barkai, N., 2002. Robustness of the BMP morphogen gradient in *Drosophila* embryonic patterning. Nature 419, 304–308.

Eldar, A., Rosin, D., Shilo, B.Z., Barkai, N., 2003. Self-enhanced ligand degradation underlies robustness of morphogen gradients. Dev. Cell 5, 635–646.

Eldar, A., Shilo, B.Z., Barkai, N., 2004. Elucidating mechanisms underlying robustness of morphogen gradients. Curr. Opin. Genet. Dev. 14, 435–439.

Entchev, E.V., Schwabedissen, A., Gonzalez-Gaitan, M., 2000. Gradient formation of the TGF-beta homolog Dpp. Cell 103, 981–991.

Esko, J.D., Lindahl, U., 2001. Molecular diversity of heparan sulfate. J. Clin. Invest. 108, 169–173.

Franch-Marro, X., Marchand, O., Piddini, E., Ricardo, S., Alexandre, C., Vincent, J.P., 2005. Glypicans shunt the Wingless signal between local signalling and further transport. Development 132, 659–666.

Fujise, M., Izumi, S., Selleck, S.B., Nakato, H., 2001. Regulation of dally, an integral membrane proteoglycan, and its function during adult sensory organ formation of *Drosophila*. Dev. Biol. 235, 433–448.

Giraldez, A.J., Copley, R.R., Cohen, S.M., 2002. HSPG modification by the secreted enzyme Notum shapes the Wingless morphogen gradient. Dev. Cell 2, 667–676.

Goodwin, G.C., Graebe, S.F., Salgado, M.E., 2001. Control System Design. Prentice Hall, New York.

Han, C., Yan, D., Belenkaya, T.Y., Lin, X., 2005. *Drosophila* glypicans Dally and Dally-like shape the extracellular Wingless morphogen gradient in the wing disc. Development 132, 667–679.

Held, L.I.J., 2002. Imaginal Discs: Thr Genetic and Cellular Logic of Pattern Formation. Cambridge Univ. Press, Cambridge, UK.

Jackson, S.M., Nakato, H., Sugiura, M., Jannuzi, A., Oakes, R., Kaluza, V., Golden, C., Selleck, S.B., 1997. dally, a *Drosophila* glypican, controls cellular responses to the TGF-beta-related morphogen, Dpp. Development 124, 4113–4120.

Kerszberg, M., Wolpert, L., 1998. Mechanisms for positional signalling by morphogen transport: a theoretical study. J. Theor. Biol. 191, 103–114.

Kirkpatrick, C.A., Dimitroff, B.D., Rawson, J.M., Selleck, S.B., 2004. Spatial regulation of Wingless morphogen distribution and signaling by Dally-like protein. Dev. Cell 7, 513–523.

Kreuger, J., Lindahl, U., Jemth, P., 2003. Nitrocellulose filter binding to assess binding of glycosaminoglycans to proteins. Methods Enzymol. 363, 327–339.

Kreuger, J., Perez, L., Giraldez, A.J., Cohen, S.M., 2004. Opposing activities of Dally-like glypican at high and low levels of Wingless morphogen activity. Dev. Cell 7, 503–512.

Lander, A.D., Nie, Q., Wan, F.Y., 2002. Do morphogen gradients arise by diffusion? Dev. Cell 2, 785–796.

Lawrence, P.A., Struhl, G., 1996. Morphogens, compartments, and pattern: lessons from *Drosophila*? Cell 85, 951–961.

Levin, M.D., Shimizu, T.S., Bray, D., 2002. Binding and diffusion of CheR molecules within a cluster of membrane receptors. Biophys. J. 82, 1809–1817.

Lin, X., Perrimon, N., 1999. Dally cooperates with *Drosophila* Frizzled 2 to transduce Wingless signalling. Nature 400, 281–284.

Lin, X., Perrimon, N., 2000. Role of heparan sulfate proteoglycans in cell-cell signaling in *Drosophila*. Matrix Biol. 19, 303–307.

Marois, E., Mahmoud, A., Eaton, S., 2006. The endocytic pathway and formation of the Wingless morphogen gradient. Development 133, 307–317.

Nolo, R., Abott, L.A., Bellen, H.J., 2000. Senseless, a Zn finger transcription factor is necessary and sufficient for sensory organ development in *Drosophila*. Cell 102, 349–362.

Orsulic, S., Peifer, M., 1996. Cell–cell signalling: Wingless lands at last. Curr. Biol. 6, 1363–1367.

Pellegrini, L., Burke, D.F., von Delft, F., Mulloy, B., Blundell, T.L., 2000. Crystal structure of fibroblast growth factor receptor ectodomain bound to ligand and heparin. Nature 407, 1029–1034.

Perrimon, N., Bernfield, M., 2000. Specificities of heparan sulphate proteoglycans in developmental processes. Nature 404, 725–728.

Rives, A.F., Rochlin, K.M., Wehrli, M., Schwartz, S.L., DiNardo, S., 2006. Endocytic trafficking of Wingless and its receptors, Arrow and DFrizzled-2, in the *Drosophila* wing. Dev. Biol. 293, 268–283.

Selleck, S.B., 2001. Genetic dissection of proteoglycan function in *Drosophila* and *C. elegans*. Semin. Cell Dev. Biol. 12, 127–134.

Seto, E.S., Bellen, H.J., 2004. The ins and outs of Wingless signaling. Trends Cell Biol. 14, 45–53.

Seto, E.S., Bellen, H.J., 2006. Internalization is required for proper Wingless signaling in *Drosophila melanogaster*. J. Cell Biol. 173, 95–106.

Strigini, M., Cohen, S.M., 2000. Wingless gradient formation in the *Drosophila* wing. Curr. Biol. 10, 293–300.

Tabata, T., Takei, Y., 2004. Morphogens, their identification and regulation. Development 131, 703–712.

Tsuda, M., Kamimura, K., Nakato, H., Archer, M., Staatz, W., Fox, B., Humphrey, M., Olson, S., Futch, T., Kaluza, V., Siegfried, E., Stam, L., Selleck, S.B., 1999. The cell-surface proteoglycan Dally regulates Wingless signalling in *Drosophila*. Nature 400, 276–280.

Yayon, A., Klagsbrun, M., Esko, J.D., Leder, P., Ornitz, D.M., 1991. Cell surface, heparin-like molecules are required for binding of basic fibroblast growth factor to its high affinity receptor. Cell 64, 841–848.